Nanostructures

The Role of Precursor-Decomposition Kinetics in Silicon-Nanowire Synthesis in Organic Solvents**

*Doh C. Lee, Tobias Hanrath, and Brian A. Korgel**

The "bottom-up" chemical synthesis of semiconductor nanowires has been developed as an alternative strategy to conventional lithographic patterning for the preparation of functional nanostructures suitable for applications such as logic gates,[1] memory devices,[2] light-emitting devices,[3] sensors,[4] and photonic circuits.[5,6] Nanowire growth by the vapor–liquid–solid (VLS) mechanism has been very successful for a variety of different materials, including Group IV, Group II–VI, and Group III–V semiconductors,[7–12] and metal oxides.[13] These nanowires are in many ways like macromolecules, as they can be suspended in solvents and deposited on substrates or mixed with polymers as composites. Ideally, the aim is to synthesize nanowires by solution chemistry and move away from slow and expensive gas-phase chemical vapor deposition (CVD).

The colloidal synthesis of Si nanomaterials is extremely challenging and represents to some extent a "holy grail" in solution-based nanomaterials chemistry. In 2000, we showed that crystalline Si nanowires could be synthesized in solution by using Au nanocrystals as seeds to lower the crystallization barrier and promote crystalline nanowire growth.[14] By pressurizing the organic solvent, reaction temperatures exceeding the Au/Si eutectic temperature (363 °C) could be reached[15] and "VLS-like" nanowire growth could be promoted. We refer to this nanowire-growth mechanism as supercritical fluid–liquid–solid (SFLS) synthesis.[16]

In hindsight, we were very lucky to stumble across diphenylsilane as a suitable Si precursor for the synthesis. Very little is known about the chemistry of the relevant silanes (that is, aryl- and alkyl-substituted silanes and trisilane) in pressurized solvents at high temperature, and as we show herein, other potential precursors that would appear to be obvious choices fail completely. In fact, we have found that the SFLS process is very sensitive to the precursor-decomposition kinetics, and careful tuning of this process is required to optimize the nanowire quality and prevent unwanted homogeneous Si-particle nucleation. Herein, we report on the relationship between the silane decomposition chemistry and the quality of the Si nanowires produced by SFLS by using Au-nanocrystal seeds.

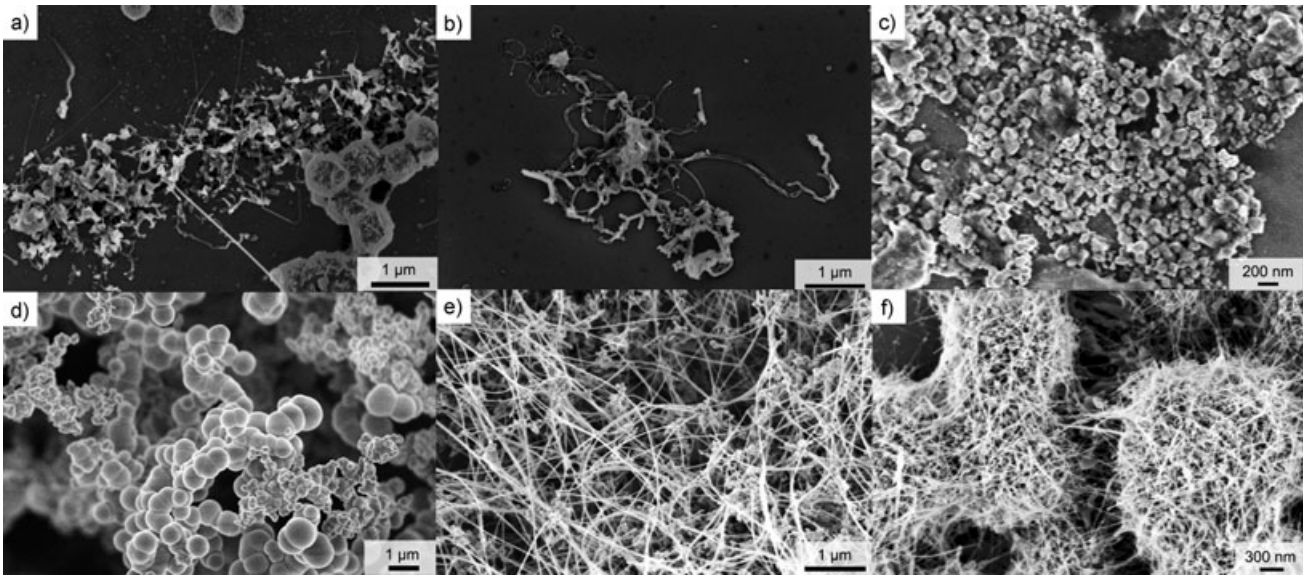

Figure 1. HRSEM images of the reaction products obtained from a) octylsilane, b) diethylsilane, c) tetraethylsilane, d) trisilane, e) phenylsilane, and f) diphenylsilane injected into hexane at 450 °C, approximately 7.2 MPa, and a concentration of 350 mM. The reactions were carried out for 5 min with a Au/Si molar ratio of 1:1000.

Figure 1 shows scanning electron microscopy (SEM) images of the solid product obtained from six different Si precursors injected into anhydrous hexane at 450 °C and 7.2 MPa with dodecanethiol-coated Au nanocrystals with an average diameter of approximately 4 nm. The silane concentration in each case was 350 mM with a Au/Si molar ratio of 1:1000, and the reactions were carried out for 5 min. The

[*] D. C. Lee, T. Hanrath, Prof. B. A. Korgel
Department of Chemical Engineering
Texas Materials Institute
Center for Nano- and Molecular Science and Technology
The University of Texas at Austin
Austin, TX 78712-1062 (USA)
Fax: (+1) 512-471-7060
E-mail: korgel@mail.che.utexas.edu

[**] This work was supported financially by the National Science Foundation, the Welch Foundation, and the Advanced Materials Research Center in collaboration with International SEMATECH. We acknowledge fruitful discussions with A. E. Saunders and thank J. P. Zhou for assistance with the high-resolution transmission electron microscopy.

 DOI: 10.1002/ange.200463001

images in Figure 1 show the products obtained from the alkyl silanes octylsilane, diethylsilane, and tetraethylsilane (Figure 1 a–c, respectively). In all cases, the nanowire was formed in extremely low yield or not at all. Only the monosubstituted alkyl silane, octylsilane, produced a measurable amount of crystalline Si nanowires, but in miniscule yield and with large amounts of oligomeric silicon- and carbon-containing impurities. The multisubstituted alkyl silanes, diethylsilane and tetraethylsilane, did not produce any crystalline nanowires, only curly amorphous wires in the case of diethylsilane and amorphous particulates in the case of tetraethylsilane. It appears that the Si–H bond is relatively reactive and labile, but homolytic cleavage of the alkyl Si–C bond is too slow to provide sufficient Si atoms for the Au-seed particles to sustain crystalline nanowire growth.

Trisilane is very reactive and decomposes rapidly at temperatures above 350 °C to produce silicon in nearly 100 % yield.[17] However, trisilane does not form Si nanowires in the presence of the Au nanocrystals. The reaction produces micrometer-sized amorphous Si colloids (Figure 1 d); surprisingly, the same product was obtained in the absence of Au nanocrystals.[18] Unlike the alkyl or aryl silane precursors, trisilane can undergo thermolysis through heterogeneous insertion at hydrogen-terminated sites on Si surfaces, which is a process that can lead to rapid particle formation once amorphous Si colloids have nucleated.[19] Furthermore, the Si–Si bonds in trisilane are very stable and do not dissociate at the typical SFLS reaction temperatures of approximately 450–500 °C. Therefore, dehydrogenation of trisilane at these reaction temperatures leaves a "bare" Si trimer, which appears not to dissolve in the Au-nanocrystal seeds. Trisilane can also be deposited on the sidewalls of any nanowires that have not fully formed to give rise to a thick amorphous coating. The alkyl silanes are not sufficiently reactive to produce high-quality crystalline nanowires by Au-seeded SFLS and trisilane is too reactive, which leads to the homogeneous particle formation of amorphous Si structures.

Aryl silanes exhibit suitable reactivity for the formation of high-quality nanowires. Figure 1 e,f shows the Si products obtained from phenylsilane and diphenylsilane: Both precursors yield large quantities of Si nanowires as the primary reaction product. As shown in Figure 2, the nanowires formed by using diphenylsilane as the precursor are crystalline with a diamond cubic structure and few defects. The alkyl- and aryl-substituted organosilanes exhibit qualitatively different reactivities at approximately 450 °C. The Si–C bonds in the alkyl-substituted silanes have lower dissociation enthalpies than those in the aryl-substituted silanes;[20,21] however, the aryl-substituted silanes can undergo disproportionation reactions of the type shown in Scheme 1, and therefore the aryl group is a more reactive substituent under the nanowire growth conditions.[22,23] Although the exact details of the disproportionation reactions have not been well-studied,[24] the mechanism appears to be associative and involves the exchange of a hydrogen atom and a phenyl group. The resonance effect of the benzene ring lowers the activation energy for the disproportionation reaction, whereas the alkyl group does not give rise to a resonance effect.[23] The alkyl-substituted silanes can only decompose by homolytic dissociation, which is very slow at these temperatures; however, the aryl silanes undergo a series

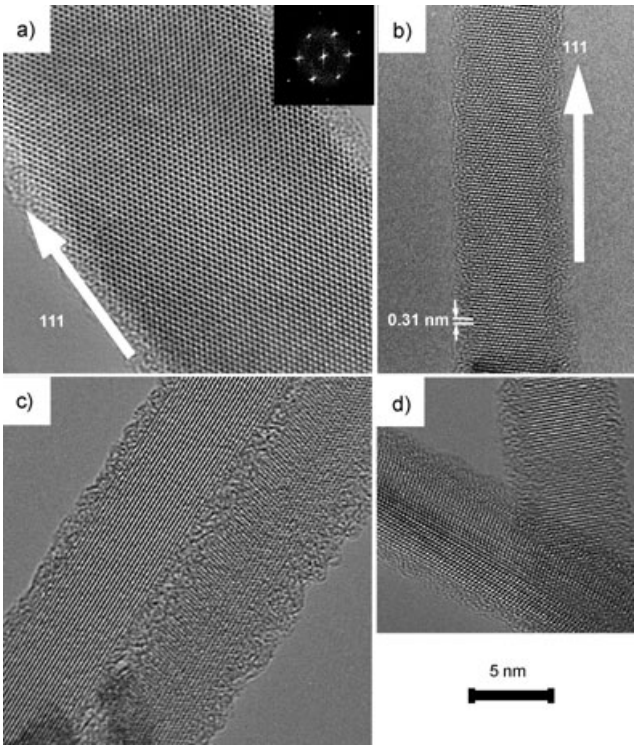

Figure 2. High-resolution TEM (HRTEM) images of Si nanowires produced by SFLS from Au nanocrystals and diphenylsilane at 450 °C. Under these conditions, SFLS yields predominantly ⟨111⟩-oriented nanowires, as shown in (a) and (b); however, limited numbers of ⟨110⟩- and ⟨211⟩-oriented nanowires are also found with diameters smaller than 10 nm (c, d). The fast Fourier transforms (FFTs) of the image in (a) are shown in the inset.

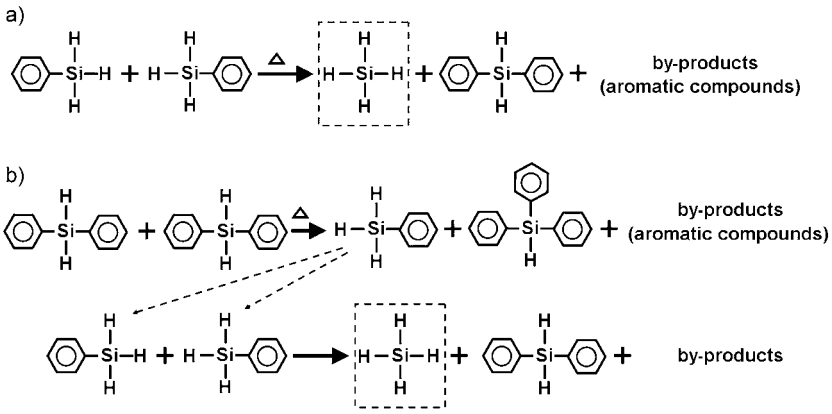

Scheme 1. Bimolecular disproportionation of a) phenylsilane and b) diphenylsilane. Silane decomposes at temperatures above approximately 350 °C to produce Si atoms.

of disproportionation reactions that yield silane and tetraphenylsilane as the final reaction products. Tetraphenylsilane is very stable and does not decompose below 500 °C,[24,25] and silane decomposes to silicon at approximately 350 °C.[26] On the basis of this proposed mechanism, silane generated in situ during the reaction promotes nanowire growth.

As expected from the proposed disproportionation mechanism for the decomposition of the aryl silanes, reactants with higher phenyl substitution give the product in lower yields. As shown in Scheme 1, phenylsilane requires only one disproportionation step to form silane, in contrast to diphenylsilane, which requires two consecutive reactions. Phenylsilane was found to lead to higher product yields than diphenylsilane. High-resolution SEM (HRSEM) analysis of the Si nanowires produced from diphenylsilane at 500 °C also showed that a significantly greater amount of carbonaceous by-products formed relative to those produced from phenylsilane. Perhaps because of its additional phenyl moiety, diphenylsilane exhibits an increased likelihood to form carbonaceous by-products as well as nanowires. For both diphenylsilane and phenylsilane, there appears to be a "threshold" concentration (approximately 120 mM for phenylsilane) below which little or no nanowire product is formed.

Figure 3 shows HRSEM images of the reaction products synthesized from phenylsilane (Figure 3a–c) and diphenylsilane (Figure 3d–e) at different reaction temperatures between 400 and 500 °C. When the synthesis was performed at 350 °C—just below the bulk-phase Si/Au eutectic temperature (363 °C)—from either phenylsilane or diphenylsilane, no significant quantities of solid product were yielded (the results are not shown). In the reactions carried out at just above the eutectic temperature (400 °C), nanowires did not form and only particulate materials that were poorly defined in structure, and so could not be clearly observed by HRSEM, were formed. This result is in stark contrast to the Au-nanocrystal-promoted SFLS synthesis of Ge nanowires, which are routinely grown at 385 °C in very high quality.[27] Since the Au/Ge system exhibits a similar eutectic temperature to that of the Au/Si system (361 °C),[27] similar results for the Si nanowires would be expected. The significantly lower growth temperature of the Ge nanowires appears to be directly related to the higher reactivity of the aryl germanes relative to the aryl silanes; therefore, the slow precursor-degradation kinetics appear to limit the Si-nanowire growth at temperatures just above the Au/Si eutectic temperature. The reaction temperature must reach approximately 450 °C

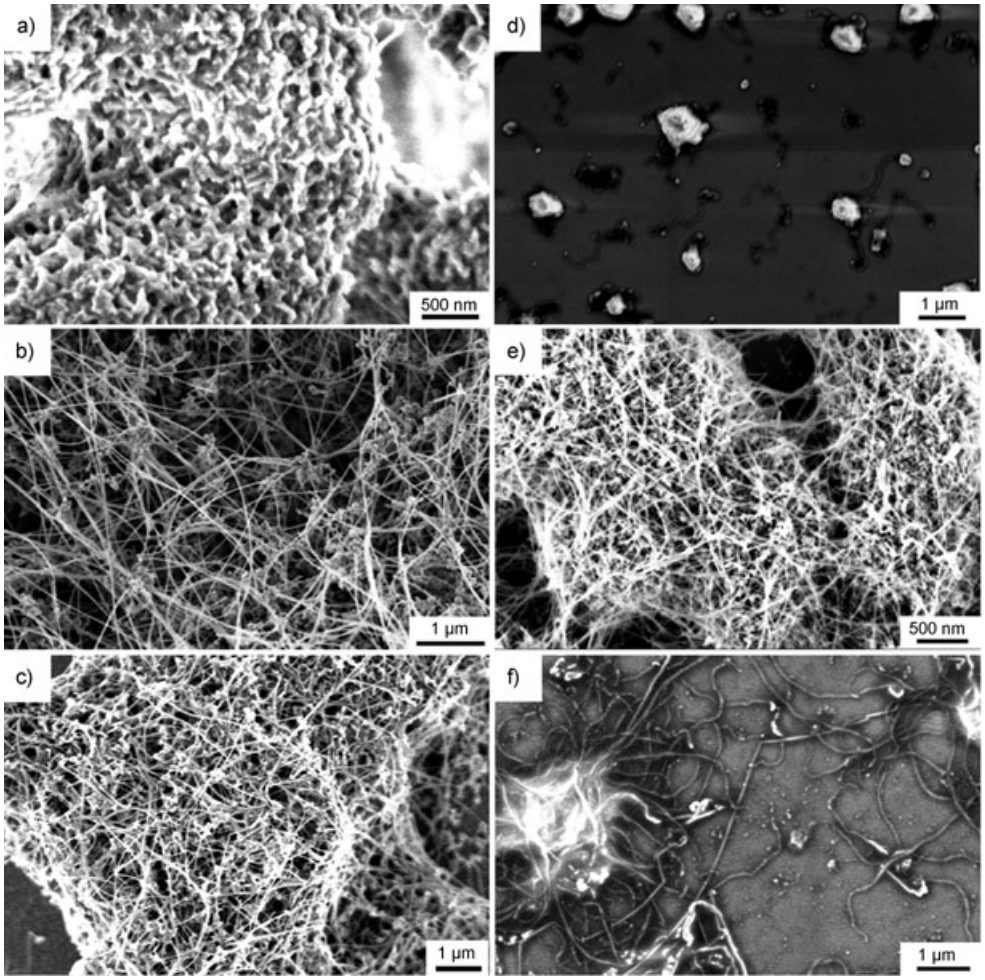

Figure 3. HRSEM images of the Si product obtained from phenylsilane (a–c) or diphenylsilane (d–f) in hexane at 400 °C (a, d), at 450 °C (b, e), and at 500 °C (c, f). For both precursors, reaction temperatures of at least 450 °C are required to form nanowires.

for high-quality crystalline Si nanowires to be produced. However, further increases in reaction temperature do not improve the nanowire growth: Phenylsilane produces nanowires at 500 °C but with a relatively high proportion of carbon-containing amorphous Si by-products, and reactions at temperatures higher than 500 °C result in significant pyrolysis of hexane.

As shown in Figures 2 and 4, ⟨111⟩ is the predominant growth direction for Si nanowires synthesized at 450 °C from Au nanocrystals and either phenylsilane or diphenylsilane. A few nanowires could be found with ⟨110⟩ or ⟨112⟩ growth directions. The preference for the ⟨111⟩ growth direction in the Si nanowires is consistent with Si whiskers grown in the gas phase by Au-seeded VLS at similar reaction temperatures.[28] Transmission electron microscopy (TEM) imaging of the Au/Si tip of the nanowires grown by SFLS reveals a flat, atomically abrupt interface with a Si (111) surface. Nanowires with ⟨112⟩ or ⟨110⟩ growth directions do not exhibit this flat cross-sectional interface (Figure 4b) but possess "curved" interfaces instead that appear to undergo reconstruction to form flat Si (111)/Au interfaces at the tip, as observed by Wu et al.[29] for Si nanowires grown by Au-seeded VLS with ⟨110⟩ orientation. The influence of the liquid–crystal interface and the fact that the Si (111)/Au interface exhibits the lowest free energy relative to other possible interfaces has been well-established from early work on Si whiskers.[28] The stability of the Si (111)/Au interface is further confirmed by our observations of a migrating Si/Au interface when it is exposed to the electron beam in TEM. Long exposure time of the Si/Au interface to the electron beam results in the generation of sufficient thermal energy for the Au interface to migrate approximately 14 nm into the nanowire (Figure 5). The interface remains sharp and atomically smooth despite this progression. Compare this interfacial structure to the curved Au/SiO_2 interface that forms at the tip of a Si nanowire after two months of exposure to air (Figure 4d). The difference in the interfacial energy of the Au/SiO_2 interface relative to the Au/Si interface is reflected in the qualitatively different structures formed.

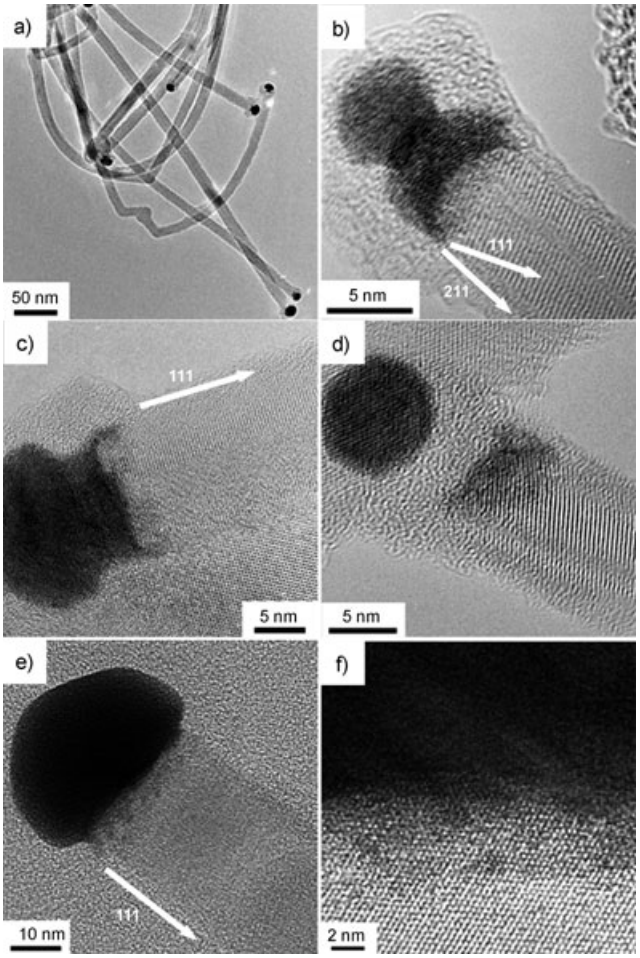

Figure 4. HRTEM images of Au-seed particles at Si-nanowire tips. a) HRTEM image of several nanowires with Au tips. b) The "curved" Au/Si interface of a ⟨211⟩-oriented nanowire. c) Au tip at the end of a ⟨111⟩-oriented Si nanowire. d) A nanowire that was exposed for two months to air that has oxidized at the Au/Si interface and the nanowire surface. e) Au tip at the end of a ⟨111⟩-oriented Si nanowire. f) The interface at the Au tip in (e) at a greater magnification of 1 000 000×.

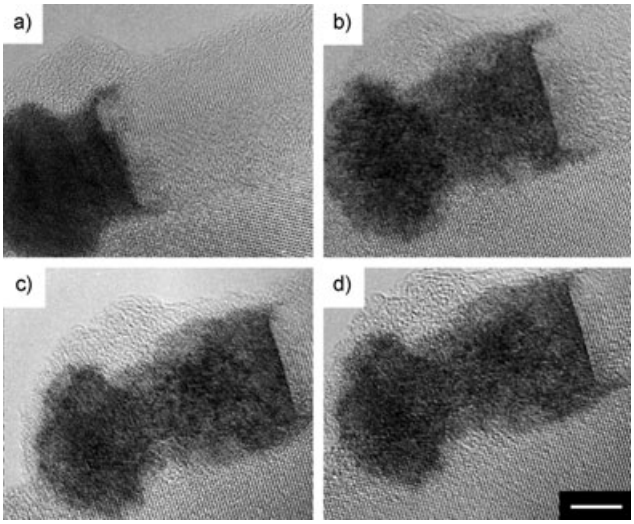

Figure 5. Au tip at the end of a Si nanowire exposed to a converged electron beam at 200 kV after a) 0, b) 1.5, c) 3, and d) 4.5 min. The Au interface migrates into the Si nanowire until it penetrates by approximately 14 nm. The nanowire maintains the sharp {111} interface at the Au/Si tip. Scale bar: 5 nm.

In summary, aryl silanes are effective precursors for the growth of crystalline Si nanowires by Au-nanocrystal-seeded SFLS, whereas alkyl silanes and trisilane are not. The quality of the Si product is related directly to the decomposition chemistry of the precursor: The precursor must be sufficiently reactive to saturate the Au-nanocrystal seeds with Si atoms and promote nanowire growth, but not so reactive that homogeneous particle nucleation and sidewall deposition overcome the metal-particle-directed crystallization. To put these findings into perspective, low-melting-point metals, such as In and Bi, have recently been used successfully as seeds to lower the metal/semiconductor eutectic temperature to below 300 °C and enable conventional solvents to be used

in the VLS method for the growth of nanowires composed of materials such as GaAs,[30] InN,[31] and CdSe.[32] For silicon nanowires, germanium nanowires, and carbon nanotubes,[33] however, the use of low-melting-point metals to lower the eutectic temperature is not a viable option because of the limited precursor reactivity for Group IV materials—even silane barely decomposes at approximately 350 °C.[21] Therefore, despite the technical challenges of high-pressure and high-temperature conditions, SFLS has an important role as a general synthetic technique for the synthesis of Group IV semiconductor nanowires.

Experimental Section

All silicon precursors (phenylsilane (Aldrich), diphenylsilane (Gelest), octylsilane (Gelest), diethylsilane (Aldrich), tetraethylsilane (Adlrich), and trisilane (Gelest)) were stored in an inert nitrogen atmosphere and were used without purification. The alkanethiol-capped Au nanocrystals were prepared according to established methods.[34] Stock solutions of the Si precursors and Au nanocrystals were prepared in anhydrous hexane in a nitrogen-filled glove box prior to injection into the reactor system.

Nanowire synthesis: The reactor system consisted of a 10-mL Ti grade-2 reaction cell, pressurized by using an HPLC pump and heated in a brass heating block.[27] The temperature was monitored with a thermocouple (Omega) that was placed on the wall of the heating block connected to a temperature controller. To help with sample collection after the reaction had been completed, an oxidized Si wafer placed inside the reactor was used as a deposition substrate (6.3 × 1.0 cm). The reactor cell was filled with anhydrous, oxygen-free hexane and sealed in a nitrogen-purged glove box. The reactor cell was connected to the high-pressure assembly and heated to the desired reaction temperature at a pressure of approximately 5.5 MPa before injection of the silane/Au nanocrystal mixture into the cell from a 500-μL HPLC injection loop. All the reactions were carried out for 5 min before careful immersion of the cell into an ice–water bath to quench the reaction. The cell was cooled to room temperature before opening. Care must be exercised when opening the reactor as it could still be under high pressure! The deposition substrate was carefully removed with sharp-edged tweezers, and the remaining product on the inner reactor walls was extracted with hexane and mild sonication. The reaction products were stored under nitrogen to minimize surface oxidation.

Characterization methods: HRSEM images were obtained on a field-emission LEO 1530 scanning electron microscope operated at an accelerating voltage of 2–3-kV. HRTEM was performed with a JEOL 2010F operated at an accelerating voltage of 200-kV. For TEM, the samples prepared by dispersion in chloroform with brief sonication followed by drop-casting on a lacey carbon grid (Electron Microscopy Sciences, LC200-Cu, Mesh 200). The nanowires were sufficiently long to stretch across the lacey carbon grid to provide a vacuum background for the HRTEM images. FFTs of the TEM images were obtained by using digital micrograph (Gatan) software.

Received: December 20, 2004
Published online: May 4, 2005

Keywords: nanowires · precursors · silicon · supercritical fluids · synthetic methods

[1] Y. Huang, X. F. Duan, Y. Cui, L. J. Lauhon, K. H. Kim, C. M. Lieber, *Science* **2001**, *294*, 1313.
[2] X. F. Duan, Y. Huang, C. M. Lieber, *Nano Lett.* **2002**, *2*, 487.
[3] M. S. Gudiksen, L. J. Lauhon, J. Wang, D. C. Smith, C. M. Lieber, *Nature* **2002**, *415*, 617.
[4] J. Hahm, C. M. Lieber, *Nano Lett.* **2004**, *4*, 51.
[5] C. J. Barrelet, A. B. Greytak, C. M. Lieber, *Nano Lett.* **2004**, *4*, 1981.
[6] F. Qian, Y. Li, S. Gradecak, D. L. Wang, C. J. Barrelet, C. M. Lieber, *Nano Lett.* **2004**, *4*, 1975.
[7] J. Westwater, D. P. Gosain, S. Tomiya, S. Usui, H. Ruda, *J. Vac. Sci. Technol. B* **1997**, *15*, 554.
[8] D. Wang, H. Dai, *Angew. Chem.* **2002**, *114*, 4977; *Angew. Chem. Int. Ed.* **2002**, *41*, 4783.
[9] T. I. Kamins, X. Li, R. S. Williams, *Nano Lett.* **2004**, *4*, 503.
[10] C. C. Chen, C. C. Yeh, C. H. Chen, M. Y. Yu, H. L. Liu, J. J. Wu, K. H. Chen, L. C. Chen, J. Y. Peng, Y. F. Chen, *J. Am. Chem. Soc.* **2001**, *123*, 2791.
[11] X. F. Duan, C. M. Lieber, *Adv. Mater.* **2000**, *12*, 298.
[12] E. A. Stach, P. J. Pauzauskie, T. Kuykendall, J. Goldberger, R. R. He, P. D. Yang, *Nano Lett.* **2003**, *3*, 867.
[13] M. H. Huang, Y. Y. Wu, H. Feick, N. Tran, E. Weber, P. D. Yang, *Adv. Mater.* **2001**, *13*, 113.
[14] J. D. Holmes, K. P. Johnston, R. C. Doty, B. A. Korgel, *Science* **2000**, *287*, 1471.
[15] C. L. Yaws, *Handbook of Thermodynamic Diagrams*, Gulf Publishing Company, Houston, Texas, **1996**.
[16] T. Hanrath, B. A. Korgel, *Adv. Mater.* **2003**, *15*, 437.
[17] A. J. Vanderwielen, M. A. Ring, H. E. Oneal, *J. Am. Chem. Soc.* **1975**, *97*, 993.
[18] L. E. Pell, A. D. Schricker, F. V. Mikulec, B. A. Korgel, *Langmuir* **2004**, *20*, 6546.
[19] M. T. Swihart, S. L. Girshick, *J. Phys. Chem. B* **1999**, *103*, 64.
[20] *Lange's Handbook of Chemistry* (Ed.: J. A. Dean), 15th ed., McGraw-Hill, New York, **1999**.
[21] L. M. Calle, A. S. Kana'an, *J. Chem. Thermodyn.* **1974**, *6*, 935.
[22] H. Gilman, D. H. Miles, *J. Org. Chem.* **1958**, *23*, 326.
[23] M. Itoh, K. Inoue, J.-I. Ishikawa, K. Iwata, *J. Organomet. Chem.* **2001**, *629*, 1.
[24] R. W. Coutant, A. Levy, *U.S. Clearinghouse Fed. Sci. Tech. Inform.*, **1969**.
[25] L. E. Nelson, N. C. Angelotti, D. R. Weyenberg, *J. Am. Chem. Soc.* **1963**, *85*, 2662.
[26] A. A. Onischuk, N. V. Panfilov, *Russ. Chem. Rev.* **2001**, *70*, 321.
[27] T. Hanrath, B. A. Korgel, *J. Am. Chem. Soc.* **2002**, *124*, 1424.
[28] A. P. Levitt in *Whisker Technology* (Ed.: A. P. Levitt), Wiley, New York, **1970**.
[29] Y. Wu, Y. Cui, L. Huynh, C. J. Barrelet, D. C. Bell, C. M. Lieber, *Nano Lett.* **2004**, *4*, 433.
[30] H. Yu, W. E. Buhro, *Adv. Mater.* **2003**, *15*, 416.
[31] S. D. Dingman, N. P. Rath, P. D. Markowitz, P. C. Gibbons, W. E. Buhro, *Angew. Chem.* **2000**, *112*, 1530; *Angew. Chem. Int. Ed.* **2000**, *39*, 1470.
[32] J. W. Grebinski, K. L. Richter, J. Zhang, T. H. Kosel, M. Kuno, *J. Phys. Chem. B* **2004**, *108*, 9745.
[33] D. C. Lee, F. V. Mikulec, B. A. Korgel, *J. Am. Chem. Soc.* **2004**, *126*, 4951.
[34] A. E. Saunders, M. B. Sigman, B. A. Korgel, *J. Phys. Chem. B* **2004**, *108*, 193.

